



Ammonoid septal formation and suture asymmetry explored with a geographic information systems approach

Margaret M. Yacobucci and Lori L. Manship

ABSTRACT

Given the centrality of suture patterns to ammonoid systematics, it is remarkable how little we understand about the formation of septa. Various models for septal formation have been proposed, but given the spatial complexity of suture patterns, the means to test and constrain them have been lacking. Here we use Geographic Information Systems (GIS) to test models for septal formation by analyzing spatial constraints and asymmetries in several ammonoid species, including Cretaceous ammonites (the Middle Turonian acanthoceratacean *Coilopoceras* and the Early Cenomanian hoplitacean *Neogastrolites*) and Carboniferous goniatites (the dimorphoceratacean *Metadimorphoceras* and the goniatacean *Somoholites*). These analyses show that suture lines are not more strongly constrained at lobe tips than at saddles, nor are lobe tips more strongly inflected than saddles. Rather, the entire suture line is similarly constrained and shaped at both lobes and saddles, suggesting that the process controlling septal folding acts along the entire margin of the septal membrane rather than at a few specified tie points. Right and left opposing sutures from the same specimens do not match precisely. More generally, right and left suture patterns show asymmetries both in lengths and degrees of variability. These asymmetries are consistent across individuals sampled from different localities, implying that they are species-level traits, rather than pathologies or taphonomic deformations. The directed asymmetry of suture patterns may reflect soft part asymmetry in ammonoids. These results can be used to place constraints on alternative models for septal growth and function; the GIS-based method will permit further testing of such models.

Margaret M. Yacobucci. Department of Geology, Bowling Green State University, 190 Overman Hall, Bowling Green, Ohio, 43403-0218, USA. mmyacob@bgsu.edu

Lori L. Manship. Department of Physical Science, University of Texas of the Permian Basin, 4901 East University, Odessa, Texas, 79762, USA. manship_l@utpb.edu

KEY WORDS: cephalopods; sutures; GIS; morphometrics; growth; constraint

INTRODUCTION

Ammonoid cephalopods are notable for their chambered shells, with the septal partitions often showing complex folding along their margins. Paleontologists have long used the suture lines formed by the intersection of the crinkled edges of the septa and the outer shell to classify ammonoids, and for more than a century have conducted various studies of suture and septal form and morphogenesis (Buckman 1892; Pfaff 1911; Spath 1919a; Westermann 1966; Mutvei 1967; Seilacher 1973; Ward and Westermann 1976; Bayer 1977a, 1977b, 1978a, 1978b; Hewitt 1985; Zaborksi 1986; Seilacher 1988; García-Ruiz et al. 1990; Hewitt et al. 1991; García-Ruiz and Checa 1993; Lutz and Boyajian 1995; Checa 1996; Checa and García-Ruiz 1996; Hammer 1999; Olóriz et al. 1999; Gildner 2003; Allen 2006) as well as their supposed function (Westermann 1971; Seilacher 1975; Westermann 1975; Henderson 1984; Hewitt and Westermann 1986, 1987; Jacobs 1990; Seilacher and LaBarbera 1995; Saunders 1995; Daniel et al. 1997; Hewitt and Westermann 1997; Hassan et al. 2002; Lewy 2002; Pérez-Claros 2005; Hammer and Bucher 2006; Pérez-Claros et al. 2007; De Blasio 2008). Given all the attention that has been paid to these features, it is surprising that we are still unsure of just how septa form or how they relate to other aspects of shell and soft part anatomy. How did the ammonoid create such a complexly folded, mineralized structure? Why are the suture lines (i.e., the folded margins of the septa) so consistently patterned that we can use sutures for fine-scale taxonomy? What process governs the addition of elements and increasing fold complexity of sutures through the ontogeny of an individual? Does the degree of sutural complexity relate to functional, constructional, developmental, or metabolic constraints on the septum?

Models for Ammonoid Septal Formation

Several models for how septa and their folded edges form have been advanced within the paleontological literature. Living *Nautilus* provides a potentially observable analog, although the details of how *Nautilus* produces its septa are still a challenge to study. When constructing a new septal plate, *Nautilus* first shifts forward in the body chamber while growing new shell around the aperture, leaving a fluid-filled gap between its soft parts and the last septum (Ward 1987). The animal secretes a new septal membrane just behind its soft parts and then begins to mineralize it. Once the new septum is partially mineralized, the fluid is removed

from the new chamber and replaced with gas (Ward 1987).

Because the septa in *Nautilus* are relatively smooth, this living analog does not offer much insight into how the pronounced folding of ammonoid septa occurs. The margins of ammonoid septa, especially those of the Jurassic-Cretaceous suborder Ammonitina, are extensively folded, producing complex suture patterns where the septum intersects the outer shell wall (Figure 1). The proposed models for ammonoid septal formation all (quite reasonably) assume that this folding occurs within the soft, organic septal membrane, before it is mineralized (Bayer 1978a). They diverge, however, in how the folds are produced and how the same pattern of folding can be produced repeatedly in each new septum as the animal grows.

Perhaps the most commonly-cited idea for septal formation is the tie-point model, best articulated by Seilacher (1973, 1975, 1988) and Westermann (1975). This model argues that the new, precalcified, septal membrane attaches to the outer shell wall at genetically defined tie-points, located at the tips of suture lobes (that is, the adapical-most flexure points; Figure 1). The membrane between the tie-points then is blown out toward the aperture by positive hydrostatic pressure, rather like a sheet pinned to a clothesline will billow out on a windy day, to form the saddles of the suture. The more tie-points present, the more complicated and crinkly the septal margin will be. The soft membrane then calcifies, preserving the crinkles and folds. Of some debate within the tie-point concept has been whether the posterior mantle of the ammonoid was involved in determining the shape of the septum (e.g., Hewitt et al. 1991), whether it was smooth or permanently fluted (e.g., Seilacher 1975 versus Westermann 1975 and Seilacher 1988), or even capable of changing form at will (Zaborksi 1986; Lewy 2002, 2003; Hewitt and Westermann 2003).

The viscous fingering model offers an alternative to the tie-point concept (García-Ruiz et al. 1990; García-Ruiz and Checa 1993; Checa and García-Ruiz 1996; Checa 2003). Here, the complex septal folding is due not to genetic constraints or the shape of the ammonoid posterior, but to the hydrostatic properties of the materials involved. Septa represent the interface between two fluids of differing viscosities, the mantle and the last, fluid-filled chamber. Such a situation will produce fractal “viscous fingering” of one fluid mass into the other; wall effects will produce greater complexity of inter-

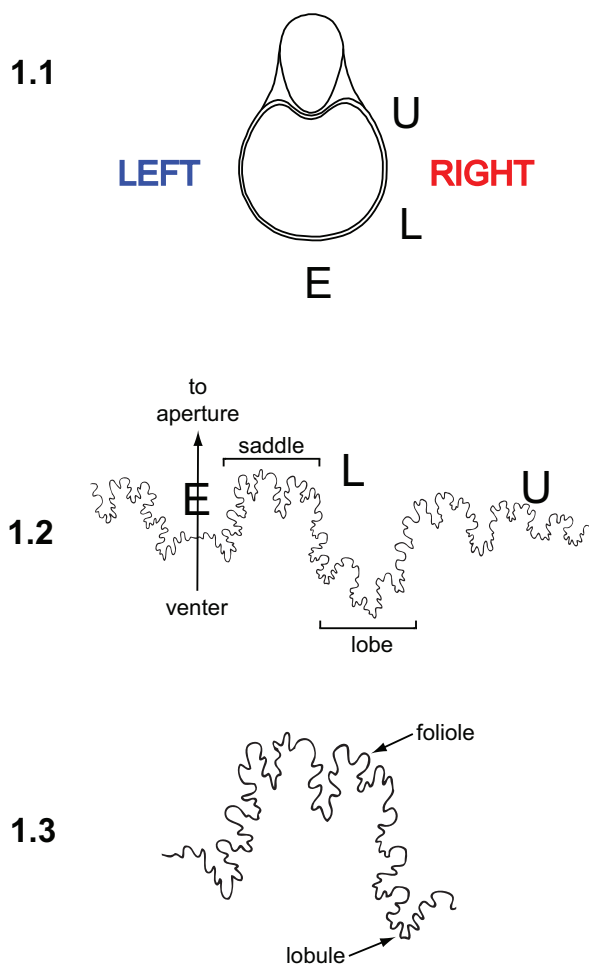


FIGURE 1. Illustration of a typical ammonite suture, with anatomical terms and orientations. 1.1 View of ammonoid shell, facing the aperture. Sutures are divided into external (E), lateral (L), umbilical (U), and internal (not shown) elements, moving from a ventral to lateral to dorsal position. Diagram of shell is redrawn and modified from Monks and Palmer (2002, p. 44). 1.2 Ammonite suture pattern with key elements labeled. The venter or outer central margin of the shell is indicated by an arrow; the arrow points toward the aperture and soft body of the animal. Note that, given this traditional orientation, the “right” suture (i.e., drawn to the right of the arrow; labeled “RIGHT” in 1.1) actually represents the left side of the ammonoid’s body. Portions of the suture line that fold up towards the aperture are called saddles; portions that fold down toward the shell apex are called lobes. Suture pattern is from *Neogastropilites muelleri*, USNM 129456, digitized from Reeside and Cobban (1960), figure 19f. 1.3 Close-up view of portion of lateral element figured in 1.2. Subfolds on saddles are termed folioles, while subfolds on lobes are termed lobules.

fingering near the shell margin and the siphuncle (García-Ruiz et al. 1990).

Hammer (1999) challenged the viscous fingering model on the grounds that a purely hydrostatic model could not produce such consistent septal forms (but see response by Checa and García Ruiz 2000). He proposed a different way to think about the problem, using a reaction-diffusion model that explored how growth of the septal membrane could be guided by interactions between a slowly diffusing activator morphogen and a more rapidly diffusing inhibitor morphogen (Hammer 1999; see also Hammer and Bucher 1999 and Guex et al. 2003 for other applications of this concept). The reactions of these molecules would be capable of producing complex (and reproducible) structures within the septal membrane without requiring direct genetic control or a complex developmental regulatory system. Hammer (1999) noted that his model was consistent with the tie-point concept, as it was concerned with understanding why specific points on the septal margin would be consistently shaped in the same way.

Careful study of ammonoid suture patterns can test some of the predictions of these models for septal formation and provide some constraints on their parameters. For example, the tie-point model implies that suture lobes should be more constrained in their position than suture saddles, and also suggests that saddle folioles should be more rounded while lobules are more incised. In addition, at least as presented by their authors, all three models make the assumption that septa are symmetrical across the shell’s dorsal-ventral midline, so that right and left suture patterns match.

To evaluate aspects like constraint and asymmetry in septal form requires a method for comparing and quantifying subtle differences in these complex structures. This paper makes use of a relatively new technique for analyzing ammonoid sutures, one that capitalizes on the power of Geographic Information Systems (GIS), to evaluate the merits of the various models for septal formation.

Geographic Information Systems (GIS) as a Morphometrics Tool

Allen (2007) provided an excellent review of previous approaches to the morphometric analysis of ammonoid sutures. She identified key reasons why suture shapes are difficult to quantify. These forms are both morphologically and mathematically complex, limiting the application of equation-based techniques such as Fourier analysis or mathematically-based simulated suture curves. Homology of

features along a suture line is difficult to assess, making the use of techniques requiring extensive inferences about homology (such as landmark-based analyses) problematic. Traditional measures of sutural fold complexity, such as fractal dimension and the suture complexity index (SCI) of Saunders (1995), can yield the same values for sutures of very different shapes and can be difficult to apply to some suture morphotypes.

Geographic Information Systems offer novel approaches to the quantitative study of anatomical form. GIS provides powerful tools for the storage, visualization, manipulation, and quantitative analysis of spatial data. While GIS is typically used to analyze geographic information, any spatially interesting phenomenon, such as an object with spatially arrayed features, is amenable to GIS techniques (Guo and Onasch 2001). In particular, many complex anatomical features of organisms, such as the occlusal surfaces of mammal molars (Zuccotti et al. 1998; Jernvall and Selänne 1999; M'Kirera and Ungar 2003; Ungar 2004; Evans et al. 2007; Plyusnin et al. 2008), conodont elements (Manship et al. 2006), and the sutures of ammonoids (Manship 2004; Waggoner and Manship 2004), are amenable to spatial analysis via GIS.

Most previous work utilizing GIS for morphometric analysis has focused on mammal teeth. As one example, Plyusnin et al. (2008) applied GIS approaches to develop an automated system for classifying mammal teeth. They used 3D surface scans to create digital elevation models (DEMs) of the teeth. Applying techniques similar to those used to study landforms, different combinations of feature selection schemes and classification models were used to find the most effective method for identifying an unknown tooth.

Manship (2004) developed a new method for inputting and analyzing ammonoid suture patterns within a GIS. This method provides a user-friendly way to compare ammonoid suture patterns visually and quantitatively as an aid to classification and the study of septal construction and function. Using GIS software, one can input, scale, and overlay suture patterns to better compare them visually. GIS technology can also pool a set of suture patterns together to make a polygon encompassing them all. This polygon represents an envelope of possible forms, useful for classifying new specimens into the correct species. The quantitative functions within GIS software enable one to calculate measures such as line lengths and areas of overlap with ease. Manship (2004) addressed the

issue of error in recording suture patterns by quantitatively comparing the same suture pattern as published in the literature and as re-recorded from the fossil specimen by herself. The quantified mismatch between the two digitized versions of the same suture pattern was substantially smaller than mismatches between different sutures, indicating that human error in tracing and flattening suture patterns is not significant relative to biologically relevant variation in suture form.

The primary advantage of GIS over more conventional morphometric tools, such as simple univariate or multivariate analyses, landmark-based approaches, eigenshape or Fourier analysis, is that GIS does not require the suture pattern to be simplified in order to quantify it. Rather than reducing a complex form to a few linear measurements, a set of landmarks, or a simplified "best-fit" curve, GIS can quantify shape in its original state, capturing the overall form of the anatomical feature being investigated and allowing for more powerful analyses. Rohlf and Marcus (1993) make a similar claim for geometric morphometrics, arguing that its ability to archive the original form of a feature makes it a more effective analytical tool than traditional multivariate morphometric techniques like principal component analysis and canonical variate analysis. However, whereas geometric morphometrics can only assess the geometric relationships among defined (and presumably homologous) landmarks, the GIS technique includes information from the entire complex form, making it potentially even more powerful for exploring shape variation.

METHODS

In order to test the proposed models for septal formation and explore variation in suture form, published suture patterns were analyzed using the GIS approach discussed above.

Ammonoid Taxa

Several ammonoid taxa representing different sutural forms were chosen for this study (Figure 2). Cretaceous ammonites with complex sutures (i.e., with many subfolds) are represented by the large Middle Turonian species *Coilopoceras springeri* (Acanthocerataceae, Coilopoceratidae; Cobban and Hook 1980) and the remarkably variable Early Cenomanian species *Neogastropilites muelleri* (Hoplitaceae, Hoplitidae; Reeside and Cobban 1960). For comparison, much simpler sutures (i.e., with few or no subfolds) from Carboniferous goniatites, including an ontogenetic sequence of *Metadimorphoceras subdivisum* (Dimorphocerataceae,

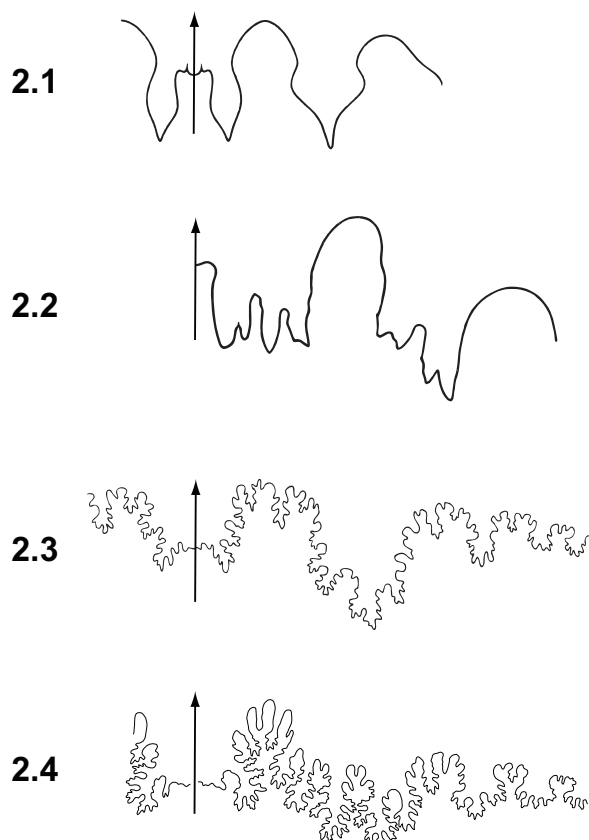


FIGURE 2. Examples of suture patterns for the four ammonoid taxa considered in this paper. Figures 2.1 and 2.2 represent goniatitic patterns while Figures 2.3 and 2.4 represent ammonitic patterns. Note that sutures are not drawn to the same absolute scale. 2.1 *Somoholites beluensis*, MTHD 12704, Saunders (1971), figure 3B, suture figured at a shell diameter of 21 mm. 2.2 *Metadimorphoceras subdivisum*, SUI 35068, Manger and Quinn (1972), figure 2F, suture figured at a shell diameter of 10.2 mm. 2.3 *Neogastropylites muelleri*, USNM 129456, Reeside and Cobban (1960), figure 19f, suture figured at a shell diameter of 65 mm. 2.4 *Coilopoceras springeri*, USNM 275917, Cobban and Hook (1980), figure 11c, suture figured at a whorl height of 50 mm (roughly 80 mm shell diameter).

Dimorphoceratidae; Manger and Quinn 1972) and five species of *Somoholites* (Goniatitaceae, Glyphyritidae; Saunders 1971; Titus and Manger 2001), were included. The selection of taxa for inclusion and the overall sample size were limited by the availability of publications that included multiple figured suture patterns per taxon. The great majority of the systematic literature for ammonoids includes only one or two figured suture patterns for each new taxon described; this paucity of suture variation data in the literature is problematic (see

Discussion below). It should be noted that the nature of the published data may produce a particular sampling bias, especially for the Paleozoic goniatites—there may have been something unusual about the taxon’s anatomy that prompted the author to include additional figures in the original monograph. Hence, the taxa included here should not be viewed as a randomly selected sample of ammonoid diversity. Institutional abbreviations: Mineralogisch Geologisch Museum Technische Hogeschool Delft (MTHD); University of Iowa (SUI); U.S. National Museum of Natural History (USNM).

Morphological Analyses in GIS

Published images of six to 20 suture patterns, depending on the taxon, were scanned as grayscale images at 600 dpi using a flatbed scanner. These published two-dimensional suture images were made by the original authors in the conventional way: by tracing the suture using a camera lucida (employing a rotating specimen mount) or tracing directly off the specimen onto a clear flexible medium (such as acetate film or plastic tape). Only right sutures of the five *Somoholites* spp. were figured, a common practice among Paleozoic ammonoid workers (see discussion below); data for the other taxa includes both right and left sutures. (Note that, in a quirk of anatomical terminology, a “right” suture refers to a suture pattern from the ventral midline to the umbilical margin of the *left* side of the shell, from the animal’s perspective. This inconsistency results from the convention of figuring sutures from a ventral view, with the adapertural direction facing up the page; see Figure 1). Where possible, the right and left sides of the same suture were both scanned. For *C. springeri*, only adult suture patterns were included. For the other taxa, available figured sutures were from juvenile specimens (*N. muelleri*) or the developmental stage was unspecified by the author (*M. subdivisum* and *Somoholites* spp.).

Using image editing software, the scanned suture patterns were scaled to a width of 5000 pixels and saved as .jpg files. These files were then imported into the ArcGIS software system (ESRI 2007). The ArcTools digitizing tool was used to digitize *C. springeri* suture patterns, while the other taxa were digitized manually in ArcMap. These digitized lines were saved as new line features. Figure 3 illustrates the fidelity of the digitizing process; Figure 3.1 shows the output of the flatbed scanner for a suture of *N. muelleri* while Figure 3.2 shows the product of digitizing that image in ArcMap.

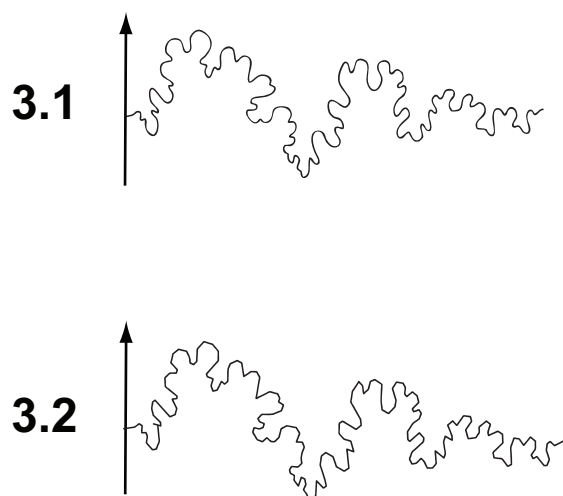


FIGURE 3. Comparison of scanned and digitized suture patterns. Suture pattern is from *Neogastrolites muelleri*, USNM 129491, Reeside and Cobban (1960), figure 19d. 3.1 Suture pattern as scanned from printed original source by flatbed scanner at 600 dpi. 3.2 Same suture pattern as in 3.1, after digitizing in ArcMap.

Once suture lines were digitized, points representing two landmarks were manually placed on each suture. These landmarks were chosen to bound the lateral sutural element, which is the most variable portion of the suture pattern for many taxa (Figure 1). Special care was taken to ensure that landmark placement was consistent within each taxon and that landmarks were placed at the precise tip (i.e., inflection point) of the bounding suture lobe. Segments of the digitized suture pattern beyond each landmark were then removed, leaving only the lateral elements. Information about the specimen (e.g., taxonomy, shell diameter, museum catalog number, publication source) was entered into the attribute table for each suture line.

Once the individual suture patterns were established in the ArcGIS environment, they could be visualized, manipulated, and compared. Sutures within each taxon were all scaled to the same arbitrary dimensions by aligning the two landmarks, using one suture pattern as the base to which others were matched. Sutures can then be overlain precisely by matching the two landmarks, allowing the suture patterns to be directly compared. It should be noted here that the scale used was specific to each taxon among the four groups included in the study, so measurements cannot be directly compared across taxa. Left sutures were scaled to each other, and also mirror-imaged in

ArcMap, so they could be aligned directly with right sutures.

As well as visual comparison, two basic types of measurements were used to compare suture patterns – lengths of suture lines and areas of polygons defined by overlapping sutures. The units of these lengths and areas are given in arbitrary units, specific to each taxon. Hence, measurements can be meaningfully compared within a taxon, but should not be compared across taxa. Suture line lengths are automatically determined by the ArcGIS software. Because each suture line segment ends at the same, fixed landmarks, the suture lengths reflect the relative degree of folding of the septal margin. In addition to suture lengths, two areas were defined. First, polygons were created that spanned the full spatial range defined by a taxon's sutures, using the ArcMap Topology-Construct tool (Figure 4). The areas of these polygons (Table 1) provide a comparative measure of the variability of suture form: more tightly constrained sutures will fill in a smaller area than sutures that are more free to vary in the path they take from one landmark to the other. Second, two suture patterns were overlain and the polygons representing mismatch of the patterns were determined (Figure 5). The summed area of these polygons (Table 2) reflects the relative degree of congruence between the two suture patterns.

To assess measurement error, one right and one left suture were selected for each taxon (two rights for *Somoholites*), and each suture was then re-digitized and rescaled five times. The lengths of the five replicate sutures were determined, as was the total area spanned by the five replicates. These replicate measures were then used to calculate the variation in length and area that can be explained solely by the measurement process (Table 3). These errors were uniformly low relative to the differences observed among different sutures.

RESULTS

Constraints

The tie-point model for septal formation implies that the position of lobe tips should be more tightly constrained than the position of saddles. In none of the ammonoids considered here was that prediction borne out. The complex, ammonitic sutures of *C. springeri* and *N. muelleri*, while showing some scatter, generally follow the same path, both through the lobes and through the saddles (Figure 4.1-4.2). The lines must all converge at the landmarks bounding the lateral element, but they

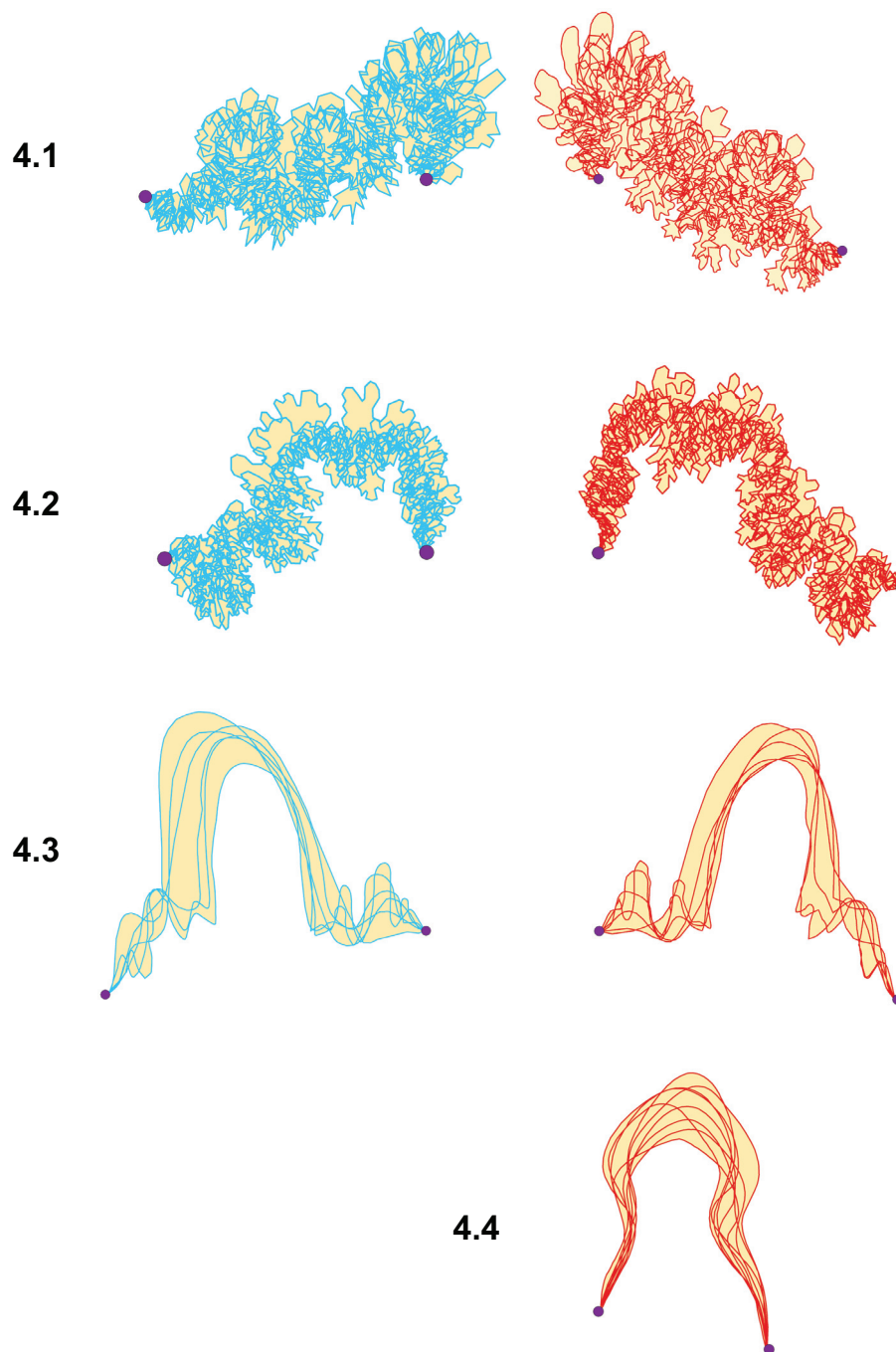


FIGURE 4. Partial suture patterns, overlain and scaled using two landmarks (purple dots) bounding the lateral element. See Table 1 for total area spanned by the sutures (represented here by the tan polygons). 4.1 *Coilopoceras springeri*. Eight left (blue) and eight right (red) lateral elements. 4.2 *Neogastrolites muelleri*. Nine left (blue) and nine right (red) lateral elements. 4.3 *Metadimorphoceras subdivisum*. Six left (blue) and six right (red) lateral elements. 4.4 *Somoholites* spp. Nine right (red) lateral elements.

remain well-aligned even far from these points. *Neogastrolites muelleri* (Figure 4.2) shows a greater degree of constraint in suture pattern than *C. springeri* (Figure 4.1), which is surprising given this species' profound intraspecific variability in

shell shape and ornamentation (Reeside and Cobban 1960). The *N. muelleri* suture patterns used here were taken from individuals chosen to represent the full range of shell forms in the species, from very compressed and lightly ornamented

TABLE 1. Area spanned by multiple overlain lateral suture elements. Note that units in this and subsequent tables are arbitrary but consistent within a taxon. Hence, comparison within a species is reasonable, while comparison between species is not. Smaller areas imply more highly constrained suture patterns; note that one side is more highly constrained than the other for each species, although which side varies by species.

Taxon	Number of Sutures Included	Left Area	Right Area
<i>C. springeri</i>	8	39.37	47.2
<i>N. muelleri</i>	9	74.1	59.2
<i>N. muelleri</i> (excluding two outliers)	7	54.7	52.1
<i>M. subdivisum</i>	6	81.9	58.8
<i>Somoholites</i> spp.	9	n/a	69.7

shells to very inflated and nodose forms. Remarkably, this shell shape variation did not produce a similar degree of sutural variation.

One might suspect that the much simpler goniatitic sutures of the Paleozoic groups might fit the tie-point model better. However, the sutures of *M. subdivisum* do not show much constraint at all, at lobes or at saddles (Figure 4.3). These sutures represent a succession of ontogenetic stages, which may account for some of the variability, especially the appearance of smaller folioles near the bounding landmarks later in ontogeny. Interestingly, the more juvenile sutures of *M. subdivisum*, which are merely scaled up here to overlain more mature patterns, have the same basic proportions and relative saddle height as the more mature ones, implying isometric growth with no apparent allometry.

Finally, *Somoholites* does show a more variably positioned saddle top, as expected under the tie-point model (Figure 4.4). However, the model can't explain the very similar positioning of the "waists" on these lines. It should be noted that these sutures come from five different species of *Somoholites*, and they still all show a very constrained pattern overall. This lack of interspecific variation probably reflects the fact that the suture pattern is so simple. Sutures like these, with a single lateral saddle element, may come closest to the ideal envisioned by the proponents of the tie-point model.

Suture Shape

An additional prediction of the tie-point model is that lobe tips should be more sharply angled, as the septal membrane bends strongly around the

tie-point, while saddle tops should be more rounded. In the Cretaceous ammonites *C. springeri* (Figure 4.1) and *N. muelleri* (Figure 4.2), the shape of both folioles and lobules (i.e., sub-folds of saddles and lobes, respectively) varies—some are gently rounded and some are more sharply incised. Among the Paleozoic goniatites, the lack of lobules in *Somoholites* prevents its use in testing this prediction, but both folioles and lobules are gently rounded in *M. subdivisum*.

Symmetry

Every proposed model for septal formation either explicitly or implicitly suggests septa should be bilaterally symmetric, with left and right sides as mirror images. Symmetry in suture patterns was therefore evaluated in *C. springeri*, *N. muelleri*, and *M. subdivisum* in several ways (only right sutures were available for *Somoholites*, so it was not included in the symmetry tests). Right (red) and left (blue) opposing sutures from the holotype of *C. springeri* are shown overlain on each other in the left side of Figure 5.1. Clearly, these patterns do not match each other very precisely. For comparison, the same right suture was overlain with a right suture from a different individual, as shown in the right side of Figure 5.1. Visually, one can conclude that right and left sides of the same septal margin are not mirror images of each other, although the mismatch is not as large as the difference between sutures from two separate individuals. The difference between pairs of sutures was quantified by defining the area of mismatch between them (yellow polygons in Figure 5). The area of mismatch for right and left sides of the same *C. springeri*

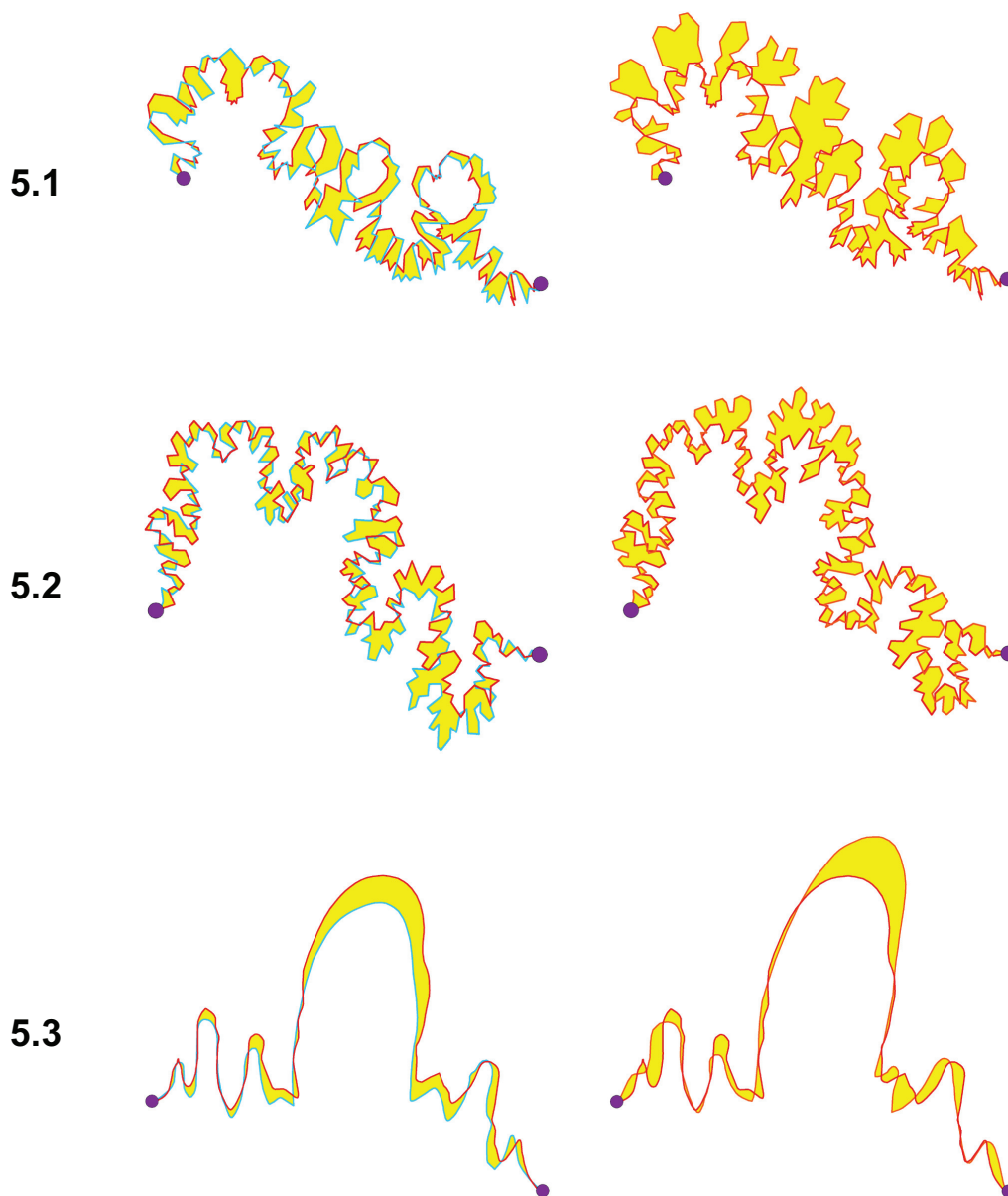


FIGURE 5. Areas of mismatch (yellow polygons) between right (red) and left (blue) sides of the same suture (left column), and between two different right sutures (right column). Note that left and right sides of the same suture pattern do not match. See Table 2 for areas of mismatch and Table 4 for individual suture lengths. 5.1 *Coilopoceras springeri*. 5.2 *Neogastrolites muelleri*. 5.3 *Metadimorphoceras subdivisum*.

suture is 9.0 units, while it is 15.3 units for two different individuals (Table 2).

Similarly, right and left sides of the same sutures are also different from each other, again to a lesser degree than those from two different individuals, in *N. muelleri* (Figure 5.2) and *M. subdivisum* (Figure 5.3). Areas of mismatch (Table 2) bear out this visual assessment.

A second way of evaluating symmetry is to compare the suture line lengths of right and left

sides of the same suture (Table 4, Figure 5). In *C. springeri*, the left side is 13% longer than the right side, while in *N. muelleri*, the right side is 2.3% longer than the left side. For comparison, this observed difference in length between right and left sides of the same suture is considerably more than that observed in replicate measurements of the same suture (<2.5% in *C. springeri* and <1.0% in *N. muelleri*; see Table 3). However, the difference in length between two right sutures from different

TABLE 2. Areas of mismatch between two lateral suture elements from the same specimen. Note that right and left sides of the same suture show mismatch, indicating that septal margins are not symmetrical across the ventral midline. For comparison, the area of mismatch of five replicates of the same suture pattern are listed in the right-hand column.

Taxon	Right vs. Left (same suture)	Right vs. Right (different sutures)	Right vs. Right (replicates of same suture)
<i>C. springeri</i>	9	15.3	0.62
<i>N. muelleri</i>	19.9	23.1	0.004
<i>M. subdivisum</i>	15.2	16.8	0.017

TABLE 3. Assessment of measurement error. For each taxon, one right and one left suture (two rights for *Somoholites*) were re-digitized and rescaled five times; the individual lengths and the area spanned by the five replicates were then determined. The 95% confidence interval (CI) for the lengths was calculated from the standard deviation of the five replicate lengths ($t_c=2.776$, $df=4$). The area spanned by the replicates can be used as an estimate of measurement error for reported areas.

Taxon	Side	95% CI for lengths	Area spanned by replicates (in square map units)
<i>C. springeri</i>	Right	0.34	0.62
<i>C. springeri</i>	Left	0.61	1.85
<i>N. muelleri</i>	Right	0.04	0.004
<i>N. muelleri</i>	Left	0.03	0.007
<i>M. subdivisum</i>	Right	0.02	0.017
<i>M. subdivisum</i>	Left	0.01	0.02
<i>Somoholites beluensis</i>	Right	0.01	0.027
<i>Somoholites deroeveri</i>	Right	0.01	0.038

specimens is larger (e.g., 42.4% difference in two *C. springeri*, 14.0% in two *N. muelleri*), indicating that inter-individual variation is larger than intra-individual asymmetry. The difference between right and left suture length is smaller in the Paleozoic *M. subdivisum*, and which side is longer varies among sutures from a single specimen.

To further explore this consistent shortening of suture patterns in the Cretaceous ammonoids, the shapes and areas spanned by multiple right or left sutures were compared (Figure 4). In *C. springeri*, for instance, the right sutures of multiple individuals are all consistently shortened relative to the left sutures, with umbilical elements displaced toward the venter (Figure 4.1). Hence, the asymmetry in

suture patterns is not merely due to a single pathological specimen. Nor can the shortening of one side relative to the other be explained by uniform post-depositional deformation, as the suture patterns come from specimens found in different localities in several states. Rather, the variation between right and left sutural line length seems to be biologically real and inherent to the species.

One can also compare how fully the right or left sutures fill in the area defined by all sutures combined. Right sutures of *C. springeri* show more scatter within this species' "template" while left sutures are more tightly aligned with each other (Figure 4.1). Therefore, for this species, left

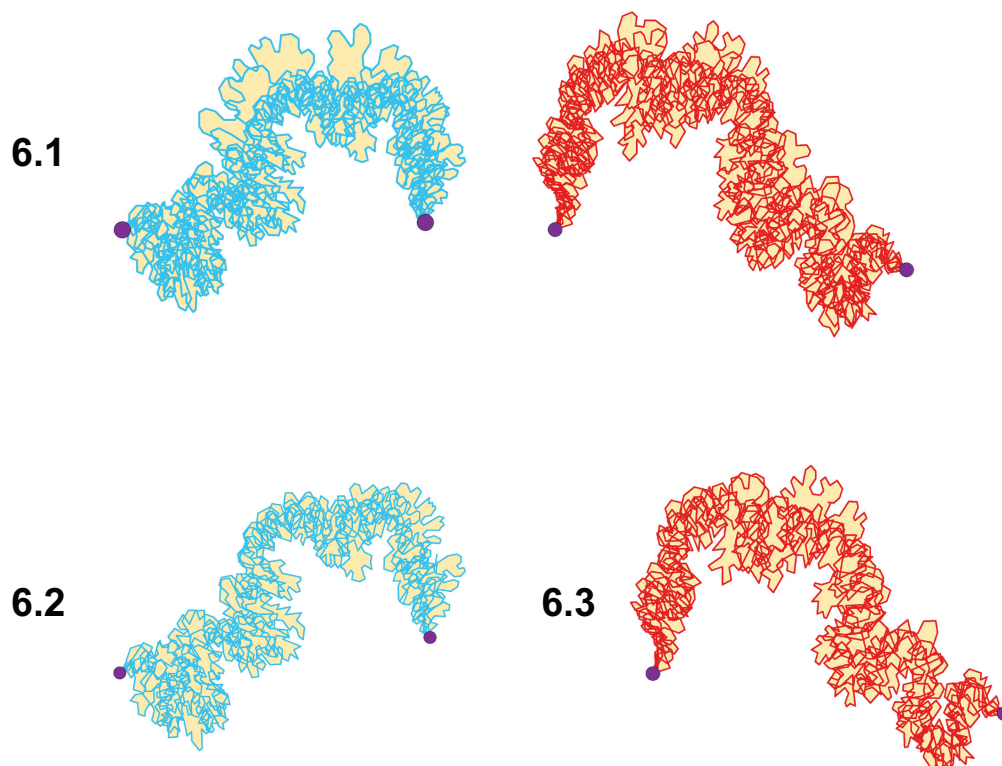


FIGURE 6. Partial sutures for *Neogastropilites muelleri*, showing the effect of two outliers with tall saddles on the total area spanned (tan polygons). 6.1 Nine left (blue) and nine right (red) lateral elements. Total areas spanned are 74.1 and 59.2 units, respectively. 6.2 Seven left lateral elements; two outliers in Figure 6.1 have been removed. Total area spanned is now 54.7 units. 6.3 Seven right partial sutures. Total area spanned is 52.1 units.

sutures appear to be more constrained in their form than right sutures.

Finally, the area spanned by sets of right versus left sutures can be compared quantitatively to assess the relative degree of variability in suture pattern. In the Paleozoic goniatite *M. subdivisum*, the right sutures appear to be notably more constrained than the lefts, based on the smaller area spanned by these lateral sutural elements relative to the same number of left elements (Table 1). This approach requires caution, however, as the selection of sutures to include in the polygon can affect the overall area spanned by the sutures. For instance, the area spanned by the eight left sutures of *C. springeri* shown in Figure 4.1 is 39.37 units while the equivalent area for the right sutures is 47.20 units (see also Table 1), supporting the visual assessment of a greater degree of constraint in left versus right sutures in this species. However, it is possible that the choice of particular sutures might produce this difference—perhaps a different set of eight right sutures would show a narrower area of coverage. To evaluate how robust this difference is to the choice of sutures to include, eight

sutures were drawn randomly from the pool of 12 right sutures that had been scanned, and the area spanned by those eight sutures was determined. This process was repeated, resulting in a total of five different subsets of eight right *C. springeri* sutures. The areas spanned by these five different polygons are listed in Table 5; the area of the left polygon is given for comparison. Note that in all five cases, the right polygon spanned a larger area than the left. To confirm this difference, the 95% confidence interval for the rights area was calculated; it is 43.13 to 53.37 units ($t_c=2.776$, $df=4$, $ci=5.12$). Since the left area falls below this interval, we can conclude that left sutures span significantly less area than right sutures. Hence, the left sutures do seem to be consistently less variable and more constrained than the right sutures in *C. springeri*.

Comparing the area spanned by left versus right sutures of *N. muelleri*, it at first appears that the opposite pattern pertains—in this species, the right sutures appear more constrained than the left sutures (Table 1). For the nine sutures shown in Figure 6.1, the area spanned by the lefts is 74.1

TABLE 4. Lengths of left versus right lateral elements of the same suture (with 95% confidence intervals based on measurement error; see Table 3). One side is longer than the other, indicating asymmetry, although which side is longer varies among the taxa.

Taxon	Left Length	Right Length
<i>C. springeri</i>	58.78±0.61	51.93±0.34
<i>N. muelleri</i>	9.28±0.03	9.49±0.04
<i>M. subdivisum</i>	5.40±0.01	5.37±0.01

TABLE 5. Area spanned by eight overlain lateral suture elements for *C. springeri*. Different sets of eight right sutures, selected randomly from a pool of 12, produce different spanned areas, but the area spanned by right sutures is always greater than that spanned by left sutures. The 95% confidence interval for the rights area is 43.13 to 53.37 ($t_c=2.776$, $df=4$, $ci=5.12$); the left area of 40.08 falls below this interval, indicating that left sutures span significantly less area than right sutures.

Polygon	Area
Left	40.08
Right 1	41.81
Right 2	47.2
Right 3	48.79
Right 4	51.01
Right 5	52.43
Mean Right	48.25
Standard Deviation Right	4.12

units while that spanned by the rights is only 59.2 units (Table 1). However, it is clear that the two sutures with very tall saddles may be acting as outliers to inflate the polygon area. Removing these two sutures to produce a polygon with seven left sutures reduces the area from 74.1 to 54.7 units (Figure 6.2, Table 1). For comparison, a polygon with seven randomly selected right sutures spans slightly less area (52.1 units; Figure 6.3, Table 1). Creating additional randomly selected subsets of seven right sutures allows the calculation of a 95% confidence interval for the area spanned by right sutures; it is 50.1 to 56.9 ($t_c=2.776$, $df=4$, $ci=3.42$). The mean for left sutures, 54.7 units, falls within this interval. Hence, after excluding the two outliers among the left sutures, no significant difference in area spanned, and therefore constraint, between the two sides remains.

DISCUSSION

These results do not provide support for the tie-point model of septal formation. Suture lobes are not more constrained in their position than suture saddles, nor are saddle tops more rounded than lobe tips, as predicted by the tie-point model (Seilacher 1973, 1975, 1988; Westermann 1975). Rather, sutures show constraint along the entire septal margin, implying that whatever controls septal shape affects the entire margin equally.

In addition, the widely assumed symmetry of suture patterns across the ammonoid's midline simply does not exist. Sutural asymmetry, while not extreme, is the norm and must be taken into account by those proposing alternative models of septal formation, such as the viscous fingering (García-Ruiz et al. 1990; García-Ruiz and Checa

1993; Checa and García-Ruiz 1996; Checa 2003) and diffusion-reaction (Hammer 1999) models. The lack of symmetry may be especially distressing for Paleozoic ammonoid workers, who, by tradition, invert drawings of left sutures so that only “rights” are figured for publication (Mapes, personal commun., 2003). Indeed, we found it difficult to locate published drawings of left sutures for Paleozoic goniatites. Hopefully, the results of the present work will encourage all ammonoid workers to specify whether they are figuring a right or a left suture pattern, and ideally figure both sides of an individual suture. We also urge paleontologists to include multiple sutures for each taxon in figures, and especially an ontogenetic series for each species, with sutures from multiple individuals at about the same ontogenetic stage included. Including more information about suture variation in the paleontological literature would greatly benefit analyses like those presented here and help us develop and test models for septal formation.

The sutural asymmetries may reflect fundamental asymmetries of the shell and/or soft parts. Modern cephalopods have asymmetrical reproductive and digestive systems (largely located in the area just in front of the septum in *Nautilus*) and even sometimes grow one eye much larger than the other (Nesis 1987; Ward 1987), so it is certainly biologically plausible for asymmetries to exist in ancient cephalopods. Indeed, numerous other authors have noted the existence of asymmetry in the suture line of ammonoids (e.g., Swinnerton and Truemann 1917; Spath 1919b; Hölder 1956; Hengsbach 1979, 1986a, 1986b; Guex and Rakus 1991; Guex 1992; Longridge et al. 2009). In most of these cases, the sutural asymmetry was produced (1) by a shift in the position of the siphuncle away from the midline, (2) as a result of a heteromorphic, helical shell shape, in which one side of the septum was enlarged relative to the other, or (3) in response to shell damage or other individual pathology. None of these explanations applies in the cases presented here. Rather, the present results suggest a more fundamental anatomical cause for the sutural asymmetry.

Notably, the asymmetry in suture pattern documented here is directed, meaning one side is consistently different from the other. Directed asymmetry (DA) is contrasted with fluctuating asymmetry (FA), in which the deviations from symmetry are randomly distributed on either side of the midline, with a mean deviation of zero when specimens are pooled (Dongen 2006). Fluctuating asymmetry has long been used as a window into

developmental instability in both extant and fossil organisms, including cephalopods (e.g., Smith 1998; Gowland et al. 2003; Dongen 2006; Vogt et al. 2008). Directed asymmetry, on the other hand, does not indicate developmental instability (Dongen 2006). However, directed asymmetry may stem from developmental regulatory mechanisms operating very early in ontogeny. Recent work has identified a potential molecular pathway, involving the transforming growth factor-beta molecule Nodal, for the establishment of left-right asymmetry in the development of snails, including the position of the initial cells of the shell gland (Grande and Patel 2009).

While the tie-point model of septal formation is not supported by the analyses presented above, the results can be used to place some constraints on alternative models for septal growth and function. One option being explored centers on work by applied mathematicians and physicists studying complexly folded thin sheets; these workers have shown how the edges of flexible membranes deform as a function of the growth rate of the membrane (Sharon et al. 2002, 2004; Marder 2003; Marder et al. 2003; Nath et al. 2003; Coen et al. 2004; Efrati et al. 2009). Applying these concepts to ammonoid septa, and relating them to Hammer's (1999) reaction-diffusion model, this model would enable septa to fold in a consistent way along their entire margin without requiring specific genetically controlled tie-points. It also blends the emphasis of the tie-point model on biological processes with the importance of considering the material properties of the septal membrane stressed by the viscous-fingering model (García-Ruiz et al. 1990; García-Ruiz and Checa 1993; Checa and García-Ruiz 1996; Checa 2003). Work is underway to develop specific predictions of this edge buckling model that can be tested using GIS-based analyses of real ammonoid sutures. Of particular interest is combining GIS and geometric morphometric techniques, such as sliding semilandmarks, to study septal surfaces in three dimensions (Bookstein 1997; Adams et al. 2004).

CONCLUSIONS

The results presented in this paper underscore our fundamental lack of understanding of septal formation in ammonoids. Why is it important to develop a sound model for the formation of septal folding in ammonoids? First, such a model may help us better understand the biological function of these folds, which has been the subject of heated debate for decades (see references in Introduc-

tion). Second, the recurrent formation of septa through ontogeny provides an especially detailed window into the growth processes of these cephalopods. The tension between developmental constraints and developmental plasticity has been suggested as a key factor in ammonoids' remarkably rapid evolutionary rates (Yacobucci 1999, 2004). Hence, by providing a way to measure and study developmental plasticity, the investigation of sutural variations may shed light on the evolutionary processes that produced such an extraordinary array of molluscan forms.

The study presented here only scratches the surface of GIS' potential as a powerful analytical tool in paleontology. GIS approaches hold great promise for addressing a wide range of questions in ammonoid paleobiology, and are also amenable to investigating the many other complex morphologies found among ancient organisms (e.g., conodonts, see Manship et al. 2006). Most earth science departments and many biology departments already hold licenses for GIS software, providing widespread access to state-of-the-art spatial analysis tools that paleontologists have only begun to exploit.

ACKNOWLEDGMENTS

The authors wish to acknowledge K. Waggoner for her many helpful suggestions, R. Mapes for guidance on Paleozoic ammonoids and ammonoid taxonomy, G. Westermann for discussions of the tie-point model, N. Levine and J. Frizado for assistance with ArcGIS, two anonymous reviewers of an earlier version of the manuscript for many insightful critiques and helpful suggestions, and A. Avruch for ideas on the text.

REFERENCES

- Adams, D.C., Rohlf, F.J., and Slice, D.E. 2004. Geometric morphometrics: ten years of progress following the 'revolution'. *Italian Journal of Zoology*, 71: 5-16.
- Allen, E.G. 2006. New approaches to Fourier analysis of ammonoid sutures and other complex, open curves. *Paleobiology*, 32:299-315.
- Allen, E.G. 2007. Understanding ammonoid sutures: New insight into the dynamic evolution of Paleozoic suture morphology. p. 159-180. In Landman, N.H., Davis, R.A., and Mapes, R.H. (eds.), *Cephalopods Present and Past: New Insights and Fresh Perspectives*. Springer, Dordrecht.
- Bayer, U. 1977a. Cephalopoden-Septen Teil 1: Konstruktionsmorphologie des Ammoniten-Septums. *Neues Jahrbuch für Geologie und Paläontologie, Abhandlungen*, 154:290-366.
- Bayer, U. 1977b. Cephalopoden-Septen Teil 2: Regelmechanismen im Gehäuse- und Septenbau der Ammoniten. *Neues Jahrbuch für Geologie und Paläontologie, Abhandlungen*, 155: 162-215.
- Bayer, U. 1978a. Constructional morphology of ammonite septa. *Neues Jahrbuch für Geologie und Paläontologie, Abhandlungen*, 157:150-155.
- Bayer, U. 1978b. The impossibility of inverted suture lines in ammonites. *Lethaia*, 11:307-313.
- Bookstein, F.L. 1997. Landmark methods for forms without landmarks: localizing group differences in outline shape. *Medical Image Analysis* 1(3):225-243.
- Buckman, S.S. 1892. A monograph of the Inferior Oolite ammonites of the British Islands, Part VII. *Monograph of the Palaeontographical Society*, 220:313-344.
- Checa, A.G. 1996. Origin of intracameral sheets in ammonoids. *Lethaia*, 29:61-75.
- Checa, A.G. 2003. Fabrication and function of ammonite septa—Comment on Lewy. *Journal of Paleontology*, 77:790-791.
- Checa, A.G., and García-Ruiz, J. M. 1996. Morphogenesis of the septum in ammonoids, p. 253-296. In Landman, N.H., Tanabe, K., and Davis, R.A. (eds.), *Ammonoid Paleobiology*. Topics in Geobiology 13. Plenum Press, New York.
- Checa, A.G., and García-Ruiz, J. M. 2000. Discussion: The development of ammonoid septa: an epithelial invagination process controlled by morphogens or by viscous fingering? *Historical Biology*, 14:299-301.
- Cobban, W.A., and Hook, S.C. 1980. The Upper Cretaceous (Turonian) Ammonite Family Coilopoceratidae Hyatt in the Western Interior of the United States. *USGS Professional Paper*, 1192:1-26.
- Coen, E., Rolland-Lagan, A., Matthews, M., Bangham, J.A., and Prusinkiewicz, P. 2004. The genetics of geometry. *Proceedings of the National Academy of Sciences (USA)*, 101: 4728-4735.
- Daniel, T.L., Helmuth, B.S., Saunders, W.B., and Ward, P.D. 1997. Septal complexity in ammonoid cephalopods increased mechanical risk and limited depth. *Paleobiology*, 23: 470-481.
- De Blasio, F.V. 2008. The role of suture complexity in diminishing strain and stress in ammonoid phragmocones. *Lethaia*, 41(1):15-24.
- Dongen, S.V. 2006. Fluctuating asymmetry and developmental instability in evolutionary biology: past, present and future. *Journal of Evolutionary Biology*, 19:1727-1743.
- Efrati, E., Sharon, E., and Kupferman, R. 2009. Elastic theory of unconstrained non-Euclidean plates. *Journal of the Mechanics and Physics of Solids*, 57(4):762-775.
- Environmental Systems Research Institute (ESRI). 2007. *ArcGIS*, ver. 9.2. Redlands, California.
- Evans, A.R., Wilson, G.P., Fortelius, M., and Jernvall, J. 2007. High-level similarity of dentitions in carnivores and rodents. *Nature*, 445:78-81.

- García-Ruiz, J.M., and Checa, A. 1993. A model for the morphogenesis of ammonoid septal sutures. *Geobios, Memoire Special*, 15:157-162.
- García-Ruiz, J.M., Checa, A., and Rivas, P. 1990. On the origin of ammonite sutures. *Paleobiology*, 16:349-354.
- Gildner, R.F. 2003. A Fourier method to describe and compare suture patterns. *Palaeontologia Electronica* 6(1):12 p., 4.1 MB; palaeo-electronica.org/2003_1/suture/issue1_03.htm.
- Gowland, F.C., Boyle, P.R., and Noble, L.R. 2003. Asymmetry in the embryonic chromatophore pattern of the squid *Loligo forbesi* (Mollusca: Cephalopoda): a proxy for developmental instability. *Journal of the Marine Biological Association of the United Kingdom*, 83: 1101-1105.
- Grande, C., and Patel, N.H. 2009. Nodal signaling is involved in left-right asymmetry in snails. *Nature*, 457:1007-1011.
- Gux, J. 1992. Origine des sauts évolutifs chez les ammonites. *Bulletin de la Société Vaudoise des Sciences Naturelles*, 82:117-144.
- Gux, J., and Rakus, M. 1991. Les Discamphiceratinae (Psiloceratidae), une nouvelle sous-famille d'ammonites (Cephalopoda) du Jurassique inférieur. *Bulletin de la Société Vaudoise des Sciences Naturelles*, 80:309-316.
- Gux, J., Koch, A., O'Dogherty, L., and Bucher, H. 2003. A morphogenetic explanation of Buckman's law of covariation. *Bulletin de la Société géologique de France*, 174:603-606.
- Guo, Y., and Onasch, C.M. 2001. Analysis of grain-scale deformation using a thin section GIS. *Geological Society of America Abstracts with Programs*, 33(6):324.
- Hammer, Ø. 1999. The development of ammonoid septa: An epithelial invagination process controlled by morphogens? *Historical Biology*, 13:153-171.
- Hammer, Ø., and Bucher, H. 1999. Reaction-diffusion processes: application for the morphogenesis of ammonoid ornamentation. *Geobios*, 32:841-852.
- Hammer, Ø., and Bucher, H. 2006. Generalized ammonoid hydrostatics modeling, with application to *Intornites* and intraspecific variation in *Amaltheus*. *Paleontological Research*, 10:91-96.
- Hassan, M.A., Westermann, G.E.G., Hewitt, R.A., and Dokainish, M.A. 2002. Finite-element analysis of simulated ammonoid septa (extinct Cephalopoda): septal and sutural complexities do not reduce strength. *Paleobiology*, 28:113-126.
- Henderson, R.A. 1984. A muscle attachment proposal for septal function in Mesozoic ammonites. *Palaeontology*, 27:461-486.
- Hengsbach, R. 1979. Zur Kenntnis der Asymmetrie der Ammoniten-Lobenlinie. *Zoologische Beiträge*, 25:107-162.
- Hengsbach, R. 1986a. Ontogenetisches Auftreten und Entwicklung der Suture-Asymmetrie bei einigen Psiloceratidae (Ammonoidea; Jura). *Senckenbergiana lethaea*, 67:323-330.
- Hengsbach, R. 1986b. Über *Arnioceras falcarius* (QUENSTEDT) und einige verwandte Arten aus Mitteleuropa (Ammonoidea; Lias). *Senckenbergiana lethaea*, 67:151-170.
- Hewitt, R.A. 1985. Numerical aspects of sutural ontogeny in the Ammonitina and Lytoceratina. *Neues Jahrbuch für Geologie und Paläontologie, Abhandlungen*, 170:273-290.
- Hewitt, R.A., and Westermann, G.E.G. 1986. Function of complexly fluted septa in ammonoid shells I. Mechanical Principles and Functional Models. *Neues Jahrbuch für Geologie und Paläontologie, Abhandlungen*, 172:47-69.
- Hewitt, R.A., and Westermann, G.E.G. 1987. Function of complexly fluted septa in ammonoid shells II. Septal evolution and conclusions. *Neues Jahrbuch für Geologie und Paläontologie, Abhandlungen*, 174:135-169.
- Hewitt, R.A., and Westermann, G.E.G. 1997. Mechanical significance of ammonoid septa with complex sutures. *Lethaia*, 30:205-212.
- Hewitt, R.A., and Westermann, G.E.G. 2003. Recurrences of hypotheses about ammonites and *Argonauta*. *Journal of Paleontology*, 77:792-795.
- Hewitt, R.A., Checa, A., Westermann, G.E.G., and Zaborski, P.M. 1991. Chamber growth in ammonites inferred from colour markings and naturally etched surfaces of Cretaceous vascoceratids from Nigeria. *Lethaia*, 24:271-287.
- Hölder, H. 1956. Über Anomalien an jurassischen Ammoniten. *Paläontologische Zeitschrift*, 30: 95-107.
- Jacobs, D.K. 1990. Sutural pattern and shell stress in *Baculites* with implications for other cephalopod shell morphologies. *Paleobiology*, 16:336-348.
- Jernvall, J., and Selänne, L. 1999. Laser confocal microscopy and geographic information systems in the study of dental morphology. *Palaeontologia Electronica* 2(1):18 p., 905KB; palaeo-electronica.org/1999_1/confocal/issue1_99.htm.
- Lewy, Z. 2002. The function of the ammonite fluted septal margin. *Journal of Paleontology*, 76: 63-69.
- Lewy, Z. 2003. Reply to Checa and to Hewitt and Westermann. *Journal of Paleontology*, 77: 796-798.
- Longridge, L., Smith, P.L., Rawlings, G., and Klaptocz, V. 2009. The impact of asymmetries in the elements of the phragmocone of Early Jurassic ammonites. *Palaeontologia Electronica* 12(1):15 p.; palaeo-electronica.org/2009_1/160/index.html.
- Lutz, T.M., and Boyajian, G.E. 1995. Fractal geometry of ammonoid sutures. *Paleobiology*, 21: 329-342.
- Manger, W.L., and Quinn, J.H. 1972. Carboniferous dimorphoceratid ammonoids from Northern Arkansas. *Journal of Paleontology*, 46:303-314.

- Manship, L.L. 2004. Pattern matching: Classification of ammonitic sutures using GIS. *Palaeontologia Electronica* Vol. 7, Issue 2; 6A: 15p, 736 KB; palaeo-electronica.org/2004_2/sutures/issue2_04.htm.
- Manship, L., Strauss, R.E., and Barrick, J. 2006. Discrimination of Frasnian (Late Devonian) *Palmatolepis* species using multivariate analysis of platform elements. *Programme & Abstracts, First International Conodont Symposium 2006 (ICOS 2006)*, Leicester, UK: 55.
- Marder, M. 2003. The shape of the edge of a leaf. *Foundations of Physics*, 33:1743-1768.
- Marder, M., Sharon, E., Smith, S., and Roman, B. 2003. Theory of edges of leaves. *Europhysics Letters*, 62:498-504.
- M'Kirera, F., and Ungar, P.S. 2003. Occlusal relief changes with molar wear in *Pan troglodytes troglodytes* and *Gorilla gorilla gorilla*. *American Journal of Primatology*, 60(2):31-41.
- Monks, N., and Palmer, P. 2002. *Ammonites*. Smithsonian Institution Press, Washington, D.C.
- Mutvei, H. 1967. On the microscopic shell structure in some Jurassic ammonoids. *Neues Jahrbuch für Geologie und Paläontologie, Abhandlungen*, 129:157-166.
- Nath, U., Crawford, B.C.W., Carpenter, R., and Coen, E. 2003. Genetic control of surface curvature. *Science*, 299:1404-1407.
- Nesis, K.N. 1987. *Cephalopods of the World: Squids, Cuttlefishes, Octopuses, and Allies*. T.F.H. Publications, Inc., Ltd., Neptune City, New Jersey. (English translation by B.S. Levitov.)
- Olóriz, F., Palmqvist, P., and Pérez-Claros, J.A. 1999. Recent advances in morphometric approaches to covariation of shell features and the complexity of suture lines in Late Jurassic ammonites, with reference to the major environments colonized, p. 273-293. In Olóriz, F., and Rodríguez-Tovar, F.J. (eds.), *Advancing Research on Living and Fossil Cephalopods*. Kluwer Academic, New York.
- Pérez-Claros, J.A. 2005. Allometric and fractal exponents indicate a connection between metabolism and complex septa in ammonites. *Paleobiology* 31(2):221-232.
- Pérez-Claros, J.A., Olóriz, F., and Palmqvist P. 2007. Sutural complexity in Late Jurassic ammonites and its relationship with phragmocone size and shape: a multidimensional approach using fractal analysis. *Lethaia* 40(3):253-272.
- Pfaff, E. 1911. Über Form und Bau der Ammoniten-septen und ihre Beziehungen zur Suturlinie. *Jahrbuch des Niedersächsischen Geologischen Vereins Hannover*, 4:207-223.
- Plyusnin, I., Evans, A.R., Karme, A., Gionis, A., and Jernvall, J. 2008. Automated 3D phenotype analysis using data mining. *PLoS One* 3(3):e1742.
- Reeside, J.B., Jr., and Cobban, W.A. 1960. Studies of the Mowry Shale (Cretaceous) and contemporary formations in the United States and Canada. *United States Geological Survey Professional Paper* 355.
- Rohlf, F.J., and Marcus, L.F. 1993. A revolution in morphometrics. *Trends in Ecology and Evolution* 8(4):129-132.
- Saunders, W.B. 1971. The Somoholitidae: Mississippian to Permian Ammonoidea. *Journal of Paleontology*, 45:100-118.
- Saunders, W.B. 1995. The ammonoid suture problem: relationships between shell and septum thickness and suture complexity in Paleozoic ammonoids. *Paleobiology*, 21:343-355.
- Seilacher, A. 1973. Fabricational noise in adaptive morphology. *Systematic Zoology*, 22:451-465.
- Seilacher, A. 1975. Mechanische Simulation und funktionelle Evolution des Ammoniten-Septums. *Paläontologische Zeitschrift*, 49:268-286.
- Seilacher, A. 1988. Why are nautiloid and ammonite sutures so different? *Neues Jahrbuch für Geologie und Paläontologie, Abhandlungen*, 177:41-69.
- Seilacher, A., and LaBarbera, M. 1995. Ammonites as Cartesian divers. *Palaaios*, 10:493-506.
- Sharon, E.B., Marder, M., and Swinney, H.L. 2004. Leaves, flowers and garbage bags: Making waves. *American Scientist*, 92:254-261.
- Sharon, E., Roman, B., Marder, M., Shin, G-S., and Swinney, H.L. 2002. Buckling cascades in thin sheets. *Nature* 419:579.
- Smith, L.H. 1998. Asymmetry of Early Paleozoic trilobites. *Lethaia*, 31:99-112.
- Spath, L.F. 1919a. Notes on ammonites I. *Geological Magazine*, 56:27-35.
- Spath, L.F. 1919b. Notes on ammonites III. *Geological Magazine*, 56:115-122.
- Swinerton, H.H., and Trueman, A.E. 1917. The morphology and development of the ammonite septum. *Quarterly Journal of the Geological Society of London*, 73:26-58.
- Titus, A.L., and Manger, W.L. 2001. Mid-Carboniferous ammonoid biostratigraphy, southern Nye County, Nevada: implications of the first North American *Homoceras*. *Paleontological Society Memoir* 55 (*Journal of Paleontology*, Supplement) 75:31.
- Ungar, P. 2004. Dental topography and diets of *Australopithecus afarensis* and early *Homo*. *Journal of Human Evolution*, 46(5):605-622.
- Vogt, G., Huber, M., Thiemann, M., van den Boogaart, G., Schmitz, O.J., and Schubart, C.D. 2008. Production of different phenotypes from the same genotypes in the same environment by developmental variation. *Journal of Experimental Biology*, 211:510-523.
- Waggoner, K.J., and Manship, L.L. 2004. Sutural variation in ammonite ontogeny: applying GIS for paleontologic analyses. *Geological Society of America Abstracts with Programs*, 36(5):422.
- Ward, P.D. 1987. *The Natural History of Nautilus*. Allen and Unwin, Boston.

- Ward, P.D., and Westermann, G.E.G. 1976. Sutural inversion in a heteromorph ammonite and its implication for septal formation. *Lethaia*, 9:357-361.
- Westermann, G.E.G. 1966. Covariation and taxonomy of the Jurassic ammonite *Sonninia adicra* (Waagen). *Neues Jahrbuch für Geologie und Paläontologie, Abhandlungen*, 124:289-312.
- Westermann, G.E.G. 1971. Form, structure, and function of shell and siphuncle in coiled Mesozoic ammonoids. *Life Science Contributions, Royal Ontario Museum*, 78:1-39.
- Westermann, G.E.G. 1975. Model for origin, function and fabrication of fluted cephalopod septa. *Paläontologische Zeitschrift*, 49:235-253.
- Yacobucci, M.M. 1999. Plasticity of developmental timing as the underlying cause of high speciation rates in ammonoids: An example from the Cenomanian Western Interior Seaway of North America, p. 59-76. In Olóriz, F., and Rodríguez-Tovar, F.J. (eds.), *Advancing Research in Living and Fossil Cephalopods*. Kluwer Academic, New York.
- Yacobucci, M.M. 2004. Buckman's paradox: Constraints on ammonoid ornament and shell shape. *Lethaia*, 37:59-71.
- Zaborski, P.M.P. 1986. Internal mould markings in a Cretaceous ammonite from Nigeria. *Palaeontology*, 29:725-738.
- Zuccotti, L.F., Williamson, M.D., Limp, W.F., and Ungar, P.S. 1998. Modeling primate occlusal topography using geographic information systems technology. *American Journal of Physical Anthropology*, 107:137-142.